Discovery of a meteoritic ejecta layer containing unmelted impactor fragments at the base of Paleocene lavas, Isle of Skye, Scotland

Simon M. Drake[1]*, Andrew D. Beard[1], Adrian P. Jones[2], David J. Brown[3], A. Dominic Fortes[4], Ian L. Millar[5], Andrew Carter[1], Jergus Baca[1] H. Downes[1]

*[1]School of Earth and Planetary Sciences, Birkbeck College, University of London, Malet St, London, WC1E 7HX, UK. (*ubseaii@mail.bbk.ac.uk)*

[2]Department of Earth Sciences, University College London, Gower St, London, WC1E 6BT, UK.

[3]School of Geographical and Earth Sciences, University of Glasgow, Lilybank Gardens, Glasgow, G12 8QQ, UK.

[4]ISIS Neutron Facility, Rutherford Appleton Laboratory, Harwell Science and Innovation Campus, Chilton, Didcot, Oxfordshire, OX11 OQX, UK.

[5]British Geological Survey, Natural Environment Research Council, Keyworth, Nottingham, NG12 5GC, UK.

*Corresponding author: Simon. M. Drake (ubseaii@mail.bbk.ac.uk)

Supplementary Data: Methods

Zircon Sample preparation and U/Pb Zircon dating (Birkbeck College/University College London, UK)

Zircons for (U/Th)He and U/Pb dating from both sample sites were isolated using conventional mineral separation techniques. Native metal phases from both sites were then separated from crushed and sieved (<300μm) sub-samples using a strong neodymium (RE) magnet, sealed in plastic film to avoid contamination and to allow easier removal of extracted magnetic grains. Separated metal phases were then prepared as polished grain mounts for analysis on the Electron Microprobe (EMP) for chemical identification.

U/Pb zircon ages from the An Carnach site were obtained using a New Wave 193 nm aperture-imaged, frequency-quintupled laser ablation system coupled to an Agilent 7700 quadrupole-based ICP-MS. A typical laser operating condition for zircon uses an energy density of ca 2.5 J/cm^2 and a repetition rate of 10 Hz. Repeated measurements of external zircon standard PLESOVIC (TIMS reference age 337.13±0.37 Ma; (Sláma, et al., 2008) and NIST 612 silicate glass (Jochum et al., 2011) are used to correct for instrumental mass bias and depth-dependent inter-element fractionation of Pb, Th and U. Temora (Black et al., 2003) and 91500 (Wiedenbeck et al., 2004) zircon were used as secondary age standards. Data are filtered using standard discordance tests with a 15% cut off. The $^{206}Pb/^{238}U$ ratio is used to determine ages where < 1100 Ma and the $^{207}Pb/^{206}Pb$ ratio for older grains. Data are processed using GLITTER 4.4 data reduction software. Time-resolved signals that record evolving isotopic ratios with depth in each crystal enabled filtering to remove spurious signals owing to overgrowth boundaries, inclusions, or fractures.

U/Pb Zircon dating for site 2 (NIGL facility, British Geological Survey, Keyworth, Nottingham, UK)

U/Pb zircon ages from the Torrin Road site were obtained using a New Wave Research UP193FX laser ablation system coupled to a Nu Instruments AttoM single-collector inductively coupled plasma mass spectrometer. Ablation parameters were optimized to suit the Pb and U contents of the material, and in all cases, bracketing reference materials were analysed using the same parameters; these were 5Hz, with a fluence of 1.5 to 3.0 J/cm2, a 30 second ablation time, and a 25 to 35 µm spot size. On the Attom, tuning was adopted that gave ThO and UO of <0.4%. Data processing for all analyses used the time-resolved function on the Nu Instruments' software, an in-house Excel spreadsheet for data reduction and error propagation, and Isoplot 4.15 for data presentation (Ludwig, 2003). Uncertainties were propagated in the manner advocated by Horstwood (2008). The Nu Attom SC-ICP-MS is used in peak-jumping mode with measurement on a MassCom secondary electron multiplier. The following masses are measured in each sweep: ^{202}Hg, ^{204}Pb+Hg, ^{206}Pb, ^{207}Pb, and^{235}U. Each data integration records 100 sweeps of the measured masses, which roughly equates to 0.22 seconds. Dwell times on each mass are 400µs on ^{207}Pb and ^{235}U, and 200µs on all other masses; the switching between masses takes 40µs. ^{238}U is calculated using^{238}U/^{235}U = 137.818.

Three zircon reference materials (91500, GJ-1 and Plesovice) were analysed at regular intervals; the bias of the ^{207}Pb/^{206}Pb and^{206}Pb/^{238}U ratios of the 91500 standard from preferred values derived by TIMS analysis are used for normalization. ^{206}Pb/^{238}U and ^{207}Pb/^{206}Pb uncertainties were propagated in a similar way utilising the measurement uncertainty and the reproducibility of the 91500 reference material. All zircons were CL-imaged prior to laser ablation work.

Ar-Ar dating (Open University, Milton Keynes, UK)

Plagioclase mineral separates were cleaned ultrasonically in acetone and then de-ionised water, dried using a hot plate and packaged in an aluminium foil packet prior to irradiation. Samples were irradiated in the 5 MW medium flux reactor at McMaster Nuclear Reactor, McMaster University, Hamilton, Ontario and analysed in the Ar-Ar and Noble Gas laboratory at the Open University. Irradiation took place in the standard 5C position with Cd shielding and for 75 MWH. Neutron flux was

monitored using biotite standard GA1550 and the J value was calculated J=0.00759 ± 0.000038, the error is included in the age calculations. Results were corrected for ^{37}Ar decay and neutron interference reactions. The following correction factors were used: $(^{39}Ar/^{37}Ar)_{Ca}$ = 0.00065 ± 0.00000325, $(^{36}Ar/^{37}Ar)_{Ca}$ = 0.000265 ± 0.00000133, and $(^{40}Ar/^{39}Ar)_{K}$ = 0.0085 ± 0.0000425, based on analyses of K and C salts.

The irradiated sample was mounted into an ultra-high vacuum system and step-heated using an SPI CW 1062 nm infra-red (IR) fibre laser. This laser was connected to a fully automated gas clean-up system, linked to a Mass Analyser Products (MAP) 215-50 noble gas spectrometer. Gas clean-up was achieved using two SAES AP10 getters, at room temperature and at 400 °C, augmented by an in-line cold-trap cooled by liquid N_2. 14 heating steps were performed in total, and blank measurements were made either side of every two heating steps. The mass discrimination value used was 283, calculated based on repeat measurements of air using an integrated calibration bottle. The age was calculated using Isoplot 3 (Ludwig, 2003) and reported at the 2σ level (including the error on J value). The data exceed the plateau criteria of at least 50% of the ^{39}Ar released in at least 4 consecutive steps (80.6% of ^{39}Ar released).

Geochronology References

Black, L. P., Kamo, S. L., Allen, C. M., Aleinikoff, J. N., David, D. W., Korsch, R. J. Foudoulis, C., 2003, Temora 1: a new zircon standard for Phanerozoic U-Pb geochronology: Chemical Geology, v. 200, p. 155-170, doi:10.1016/S0009-2541(03)00165-7.

Horstwood, M., 2008, Data reduction strategies, uncertainty assessment and resolution of LA-(MC-) ICP-MS isotope data, Mineralogical Association of Canada, v. 40, p. 283-303.

House, M.A., Farley, K.A., and Stockli, D, 2000, Helium chronometry of apatite and titanite using Nd-YAG laser heating. Earth and Planetary Science Letters, v. 183, p. 365–368.

Jochum, K. P., Weis, U., Stoll, B., Kuzmin, D., Yang, Q., Raczek, I., Jacob, D. E., Stracke, A., Birbaum, K., Frick, D. A., Günther, D. and Enzweiler, J., 2011, Determination of Reference Values for NIST SRM 610617 Glasses Following ISO Guidelines: Geostandards and Geoanalytical Research, v. 35, p. 397-425.

Ludwig, K. R., 2003, Isoplot/EX version 3.0, A geochronological toolkit for Microsoft Excel: Berkeley Geochronology Center Special Publication.

Wiedenbeck, M., Hanchar, J. M., Peck, W. H., Sylvester, P., Valley, J., Whitehouse, M., Kronz, A., Morishita, Y., Nasdala, L., Fiebig, J., Franchi, I., Girard, J.-P., Greenwood, R.C., Hinton, R., Kita, N., Mason, P.R.D., Norman, M., Ogasawara, M., Piccoli, P.M., Rhede, D., Satoh, H., Schulz-Dobrick, B., Skår, O., Spicuzza, MJ., Terada, K., Tindle, A., Togashi, S., Vennemann, T., Xie, Q. and Zheng, Y.-F., 2004, Further Characterisation of the 91500 Zircon Crystal: Geostandards and Geoanalytical Research, v. 28, p. 9–39, doi:10.1111/j.1751-908X.2004.tb01041.

Raman microscopy (University College London, UK)

Raman spectra of the reidite/zircon were acquired using a B&WTek i-Raman plus portable spectrometer, equipped with a 532 nm laser (37 mW power at the fiber-optic probe tip) to stimulate Raman scattering, which is measured in the range 170 - 4000 cm^{-1} with spectral resolution of 3 cm^{-1}.

Reidite was first discovered by high pressure experimentation (Reid and Ringwood, 1969), and was later formed by in-situ laser heating (Knittle and Williams, 1993) and shock experiments on zircon (Leroux et al., 1999). Reidite can be detected by Raman microscopy and infrared analysis (Gucsik et al., 2004) or by electron backscatter diffraction (EBSD), and focused ion beam imaging (Reddy et al., 2015; Erickson et al., 2017).

We note that slight shifts between 800 and 890 were recorded by Knittle and Williams (1993) as being due to changes in Si-O bond strength because of an increase in bond length, a change in electron density function or a charge transfer between O and Zr or O and Si. These workers used ‘transparent’ zircons during their high pressure shock experiments. It is unknown whether inclusions in natural zircons would influence band shifts in the 800-900 range when instantaneously shocked. Only five recorded terrestrial sites of natural reidite (supplementary file Tab.DR5) have been documented, ranging from 50 ka to 1.18 Ga in age (Reddy et al., 2015).

Reidite References

Erickson, T. M., Pearce, M. A., Reddy, S. M., Timms, N. E., Cavosie, A. J., Bourdet, J., Rickard W. D. A., Nemchin, A. A., 2017, Microstructural constraints on the mechanisms of the transformation to reidite in naturally shocked zircon: Contributions to Mineralogy and Petrology, v. 172(6), doi:10.1007/s00410-016-1322-0.

Gucsik, A., Koeberl, C., Brandstätter, F., Libowitzky, E. and Reimold, W. U., 2004, Cathodoluminescence, electron microscopy and Raman spectroscopy of experimentally shock metamorphosed zircon crystals and naturally shocked zircon from the Ries impact crater: *in* Dypvik, H., et al., (eds.), Cratering in marine environments and on ice: Berlin-Heidelberg, Springer, p. 281-322.

Leroux, H., Reimold, W. U., Koeberl, C., Hornemann, U., and Doukhan, J-C., 1999, Experimental shock deformation in zircon: A transmission electron microscopic study: Earth and Planetary Science Letters, v. 169, p. 291–301, doi:10.1016 /S0012 -821X (99) 00082-5.

Reddy, S. M., Johnson, T. E., Fisher, S., Rickard, W. D. A. and Taylor, R. J. M., 2015, Precambrian reidite discovered in shocked zircon from Stac Fada impactite Scotland: Geology, v. 43, p. 899-902, doi:10.1130/G37066.1.

Reid, A. F. and Ringwood, A. E., 1969, Newly observed high pressure transformations in Mn3O4, CaAl2O4, and ZrSiO4: Earth and Planetary Science Letters, v. 6, p. 205–208.

Electron microprobe analysis (Birkbeck College, London, UK)

Major elemental analyses of the native metal, sulphide and phosphide phases were obtained using a Jeol JXA8100 Superprobe (Wavelength System) and an Oxford Instruments AZtec system (Energy System) at Birkbeck College. Analysis was carried out using an accelerating voltage of 15 kV, current of 1×10^{-8} A, and a beam diameter of 1μm. Analyses were calibrated against standards of Spec-pure metals, natural sulphides, oxides and silicates, with the data corrected using a ZAF program.

Figure DR1: Individual zircon ages recovered from Skye impactoclastites and dated using laser ablation U-Pb methods. Site 1 (blue, ~80 analyses) and site 2 (red, ~87 analyses). The zircons record mostly Precambrian crystallisation ages. Note the presence of Triassic aged zircons at site 1. Their presence precludes any association with the 1.18 Ga Stac Fada event.

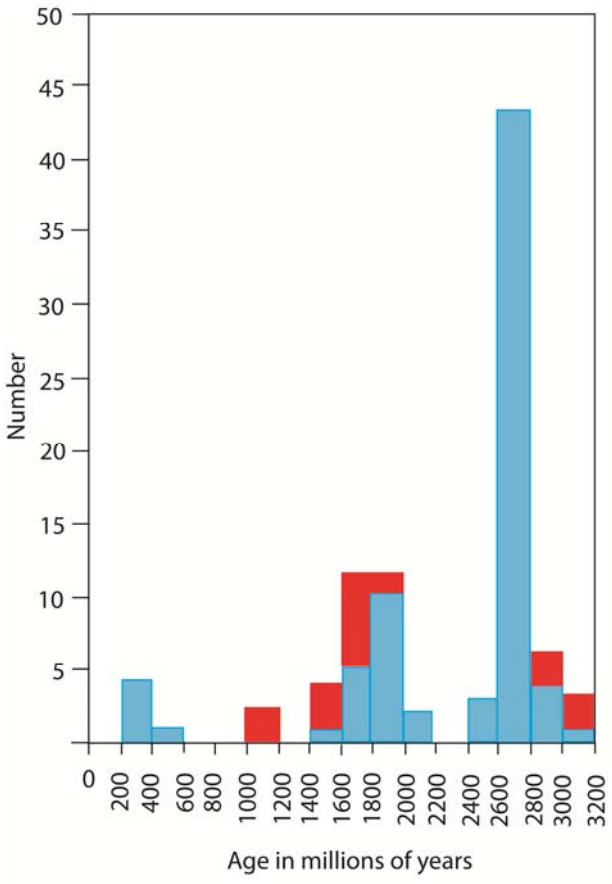

Figure DR2: Vertical logged sections of Impactoclastite deposits at site 1 and site 2.

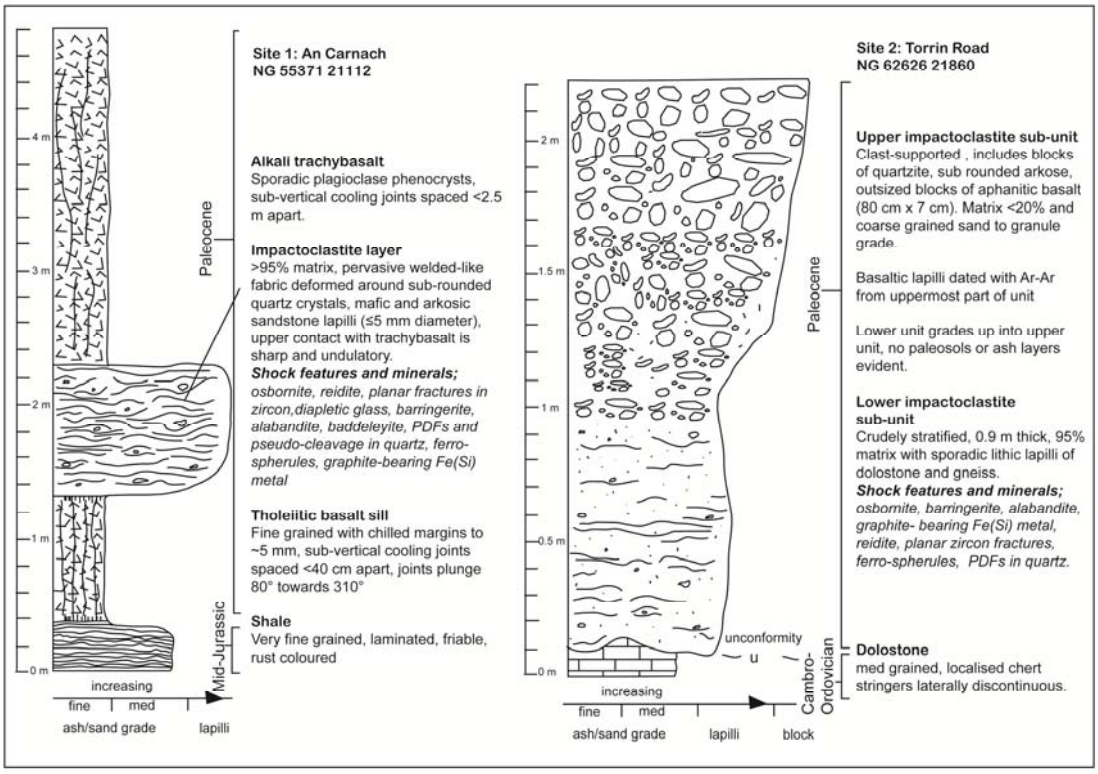

Figure DR3: Plateau age of basaltic clast incorporated in impactoclastite at site 2

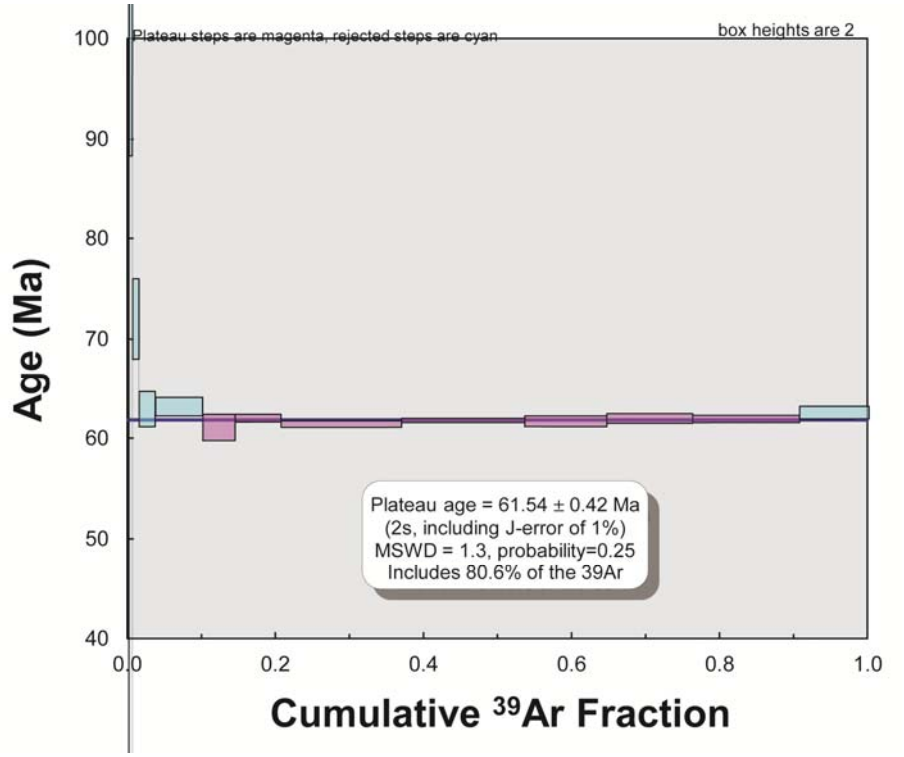

Figure DR4: Reidite peaks for site 1 and site 2 Isle of Skye together with peaks for natural zircon and synthetically derived reidite

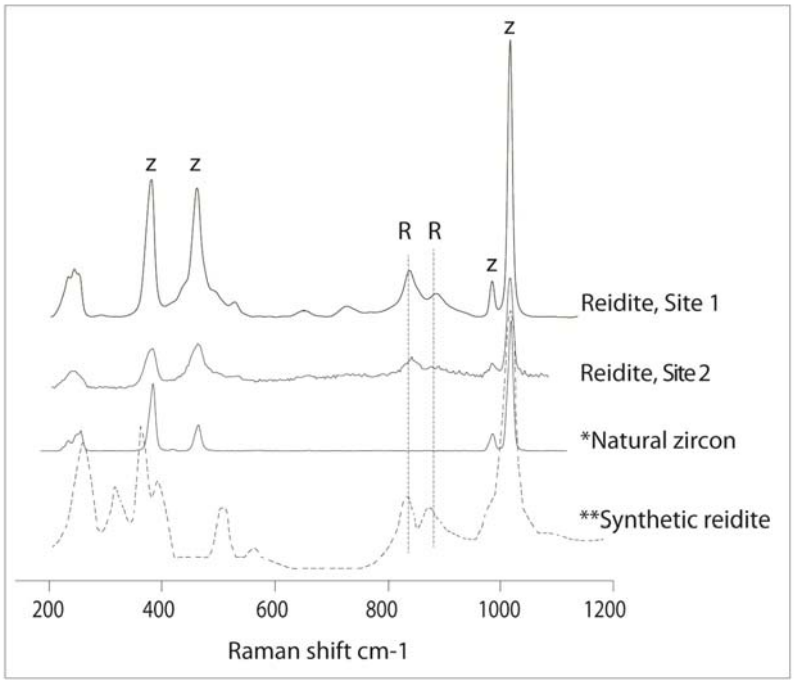

***** Knittle, E. and Williams, Q., 1993 High-pressure Raman spectroscopy of $ZrSiO_4$: Observation of the zircon to scheelite transition at 300 K: Am Mineral v. 78, p. 245–252.

****** Raman Spectrum http://rruff.info/Zircon/R050203

Figure DR5: Concordia plots of zircon ages at site 2 lower unit near the Chambered Cairn

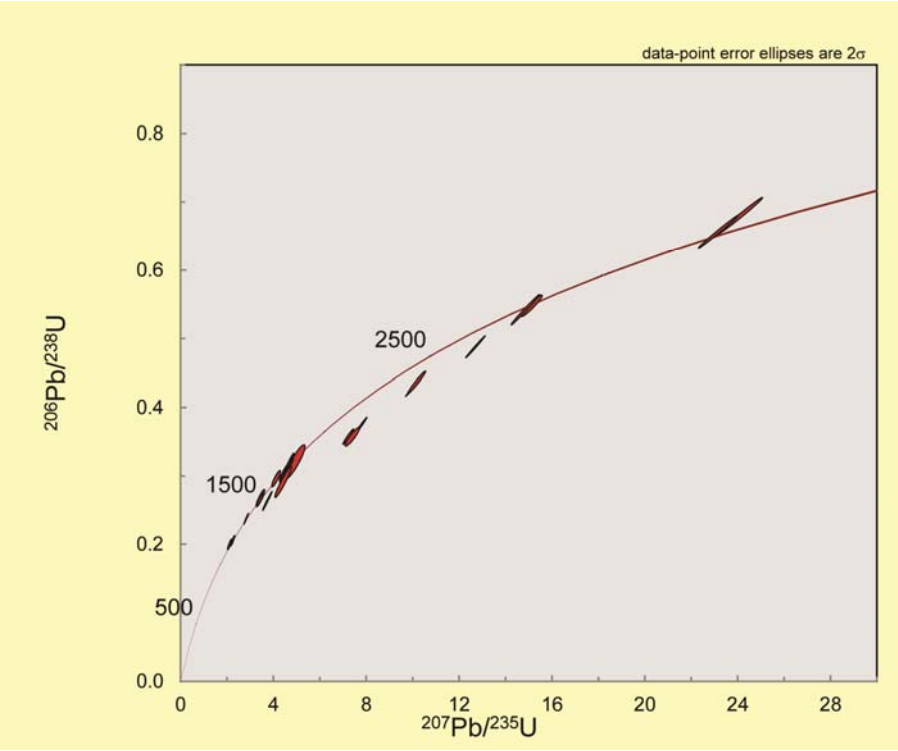

Figure DR6

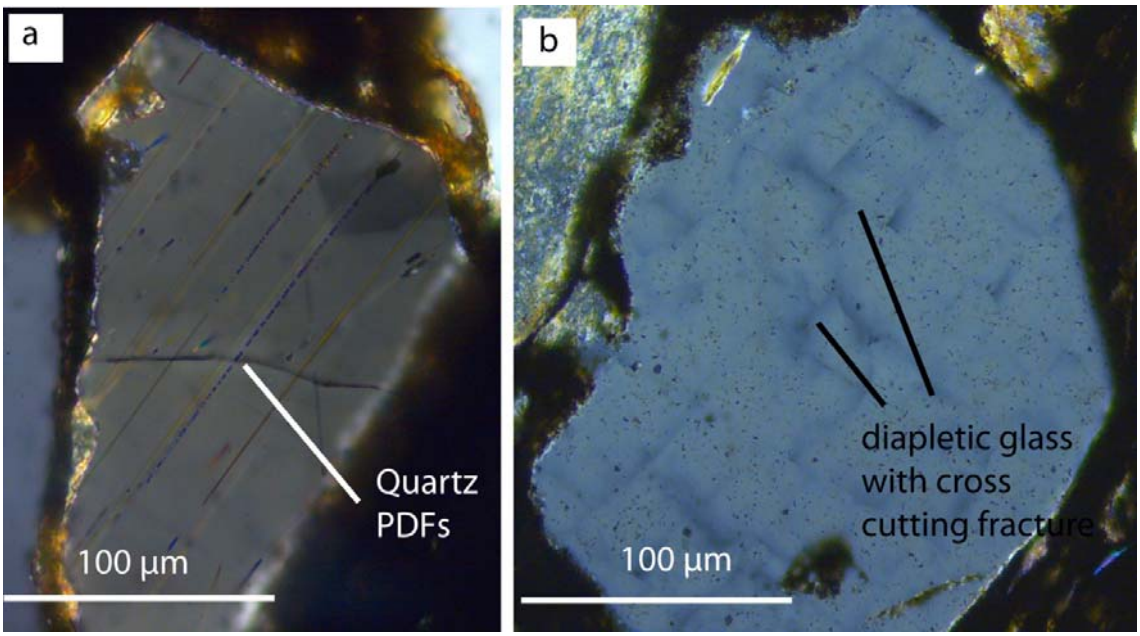

a) Quartz grain from site 1, with both fresh and decorated sets of Planar Deformation Features (PDFs). The decorated PDFs indicate some degree of re-crystallisation has occurred, with the original PDF now appearing as straight arrays of fluid inclusions.

b) Quartz grain from site 1 exhibiting Planar Fractures (PFs) forming a pseudo-cleavage with areas of diaplectic glass. Such glass commonly occurs at the PFs intersections and indicate derivation from instantaneous high pressure shock at 30–50 GPa (*French and Koeberl, 2010).

* French, B.M., and Koeberl, C., 2010 The convincing identification of terrestrial meteorite impact structures: What works, what doesn't, and why: Earth Science Reviews, v. 98, p. 123–170, doi:10.10.16/j.earscirev.2009.10.009.

Table DR1 : Step heating ages (highlighted in yellow) of basaltic clast at site 2 (near Chambered Cairn- upper unit).

J = 0.007608838

Run No	Comment	40Ar	+/-	39Ar	+/-	38Ar	+/-	37Ar	+/-	36Ar	+/-
12A62218	Step 1	0.0077206	0.0007437	3.52E-05	3.45E-05	8.47E-06	1.39E-05	0.000462	0.0002823	2.13E-05	1.19E-05
12A62219	Step 2	0.1174556	0.0007804	0.0008816	4.15E-05	6.98E-05	1.39E-05	0.0029385	0.0002824	0.0002506	1.19E-05
12A62221	Step 3	0.6037719	0.0010273	0.0162696	7.75E-05	0.0005093	2.25E-05	0.0351579	0.0002826	0.0013921	2.10E-05
12A62222	Step 4	0.826142	0.0008843	0.0416012	0.000117	0.0009488	2.25E-05	0.075171	0.0002827	0.0020415	2.10E-05
12A62224	Step 5	1.4962781	0.0014745	0.0944759	0.0002087	0.002114	3.21E-05	0.2689395	0.0002829	0.0035702	2.10E-05
12A62226	Step 6	2.8966043	0.0042113	0.2820416	0.0004146	0.0052926	5.20E-05	0.7303898	0.0002832	0.0053279	3.07E-05
12A62229	Step 7	1.4950603	0.0009783	0.1848611	0.0003527	0.0031667	4.19E-05	0.3652978	0.0002835	0.0022246	3.07E-05
12A62232	Step 8	1.6550157	0.0015328	0.2702872	0.0003831	0.0043544	5.14E-05	0.6055781	0.0002643	0.0013912	1.07E-05
12A62234	Step 9	4.2513418	0.0033718	0.7072563	0.000576	0.0107833	6.16E-05	1.4445159	0.0002645	0.0034789	3.03E-05
12A62237	Step 10	4.145167	0.0020956	0.7188705	0.0005555	0.0107833	9.21E-05	1.2374778	0.0002648	0.0028737	2.04E-05
12A62238	Step 11	2.8387972	0.0020086	0.4792595	0.0005148	0.0072878	4.12E-05	1.1179034	0.000265	0.0021854	3.03E-05
12A62240	Step 12	2.9748736	0.0030579	0.5001037	0.0001796	0.0074718	4.12E-05	1.1411486	0.0002652	0.0022793	3.03E-05
12A62241	Step 13	3.9264884	0.0044144	0.6326591	0.0008837	0.0094444	8.19E-05	1.2431118	0.0002653	0.0034522	2.04E-05
12A62243	Step 14	2.9077482	0.0022316	0.4050682	0.0006475	0.0064599	7.18E-05	1.0550581	0.0002656	0.0034721	3.03E-05

Run No	Comment	40Ar*/39Ar	+/-	Age	+/-	+/-(no J error)	39/40	+/-	36/40	+/-	37/39	+/-	38/39	+/-
12A62218	Step 1	40.522344	109.42472	484.77396	1147.9343	1147.9324	0.0045536	0.0044847	0.0027597	0.0015599	13.142534	15.178657	0.2408855	0.4595569
12A62219	Step 2	49.218082	4.6876865	573.76612	46.874215	46.809756	0.0075055	0.0003568	0.002134	0.000102	3.333262	0.3566748	0.079171	0.0161591
12A62221	Step 3	11.825921	0.3906128	155.41552	4.9745444	4.9185101	0.0269466	0.0001362	0.0023057	3.50E-05	2.1609585	0.020188	0.0313032	0.00139
12A62222	Step 4	5.3574522	0.1513975	72.070073	2.0275109	1.9965011	0.050356	0.0001516	0.0024711	2.56E-05	1.806945	0.0084871	0.0228067	0.0005443
12A62224	Step 5	4.6709877	0.0682921	62.994777	0.9565856	0.9051199	0.0631406	0.0001527	0.002386	1.42E-05	2.8466454	0.006964	0.0223757	0.0003429
12A62226	Step 6	4.688022	0.036114	63.220529	0.5705535	0.4785827	0.0973697	0.0002013	0.0018394	1.09E-05	2.5896529	0.0039368	0.0187655	0.0001863
12A62229	Step 7	4.5314231	0.0500733	61.144087	0.7291774	0.6643347	0.1236479	0.0002494	0.001488	2.05E-05	1.9760667	0.0040702	0.0171302	0.0002292
12A62232	Step 8	4.6022133	0.0145472	62.083035	0.360996	0.192901	0.163314	0.0002765	0.0008406	6.51E-06	2.2404984	0.003323	0.0161104	0.0001915
12A62234	Step 9	4.5575211	0.0140242	61.490303	0.3549279	0.186027	0.1663607	0.0001891	0.0008183	7.15E-06	2.042422	0.0017048	0.0152467	8.79E-05
12A62237	Step 10	4.5849404	0.0095625	61.853975	0.329418	0.1268188	0.1734238	0.0001601	0.0006933	4.94E-06	1.7214197	0.0013804	0.0150004	0.0001287
12A62238	Step 11	4.5758196	0.0197481	61.73301	0.4008476	0.2619171	0.1688248	0.0002171	0.0007698	1.07E-05	2.332564	0.0025656	0.0152064	8.76E-05
12A62240	Step 12	4.601749	0.0189734	62.076877	0.3954609	0.2515951	0.1681092	0.000183	0.0007662	1.02E-05	2.281824	0.0009761	0.0149405	8.27E-05
12A62241	Step 13	4.5938656	0.0134442	61.972338	0.3529409	0.1782862	0.1611259	0.0002889	0.0008792	5.29E-06	1.9648999	0.0027764	0.0149281	0.0001312
12A62243	Step 14	4.6455136	0.0239353	62.657119	0.4421306	0.3172889	0.1393065	0.000247	0.0011941	1.04E-05	2.6046435	0.0042151	0.0159477	0.000179

Table DR2: Zircon ages (highlighted in yellow) of site 1 (An Carnach) zircons

				Ratios						Ages (Ma)									
Grain No.	Pb (ppm)	U (ppm)	Atomic Th/U	206/238	± s.e.	207/235	± s.e.	207/206	± s.e.	206/238	± 2s	207/235	± 2s	207/206	± 2s	% concord. (206/238 207/235)	% concord. (206/238 207/206)	Best Age	±2s
G1	153.3	281.1	0.34	0.4989	0.0057	13.0620	0.1749	0.1900	0.0024	2609.0	49.1	2684.1	32.2	2741.7	23.9	2.8	4.8	2741.7	23.9
G2	56.1	102.1	0.45	0.4889	0.0058	12.6754	0.1891	0.1881	0.0027	2566.0	50.5	2655.8	35.2	2725.5	27.3	3.4	5.9	2725.5	27.3
G3	38.1	909.2	0.55	0.0389	0.0005	0.2879	0.0065	0.0537	0.0012	246.1	5.8	256.9	11.5	357.2	13.5	4.2	31.1	246.1	5.8
G4	152.5	236.4	0.29	0.5862	0.0068	18.9396	0.2588	0.2344	0.0030	2973.9	55.3	3038.7	33.5	3082.5	25.0	2.1	3.5	3082.5	25.0
G5	8.7	23.8	1.42	0.2705	0.0039	3.8046	0.1139	0.1021	0.0031	1543.2	40.0	1593.7	54.3	1661.9	49.8	3.2	7.1	1661.9	49.8
G6	14.3	42.0	0.23	0.3323	0.0043	5.3870	0.1112	0.1176	0.0024	1849.4	41.3	1882.8	41.7	1920.4	35.6	1.8	3.7	1920.4	35.6
G7	157.8	258.8	0.43	0.5328	0.0062	13.9589	0.1959	0.1901	0.0025	2753.1	52.2	2746.9	33.6	2743.0	25.3	-0.2	-0.4	2743.0	25.3
G8	96.4	384.6	0.32	0.2424	0.0028	3.0827	0.0449	0.0923	0.0013	1399.4	29.0	1428.4	27.6	1472.7	21.6	2.0	5.0	1472.7	21.6
G9	46.1	78.3	0.61	0.5009	0.0060	12.5955	0.1897	0.1825	0.0027	2617.5	51.4	2649.9	35.4	2675.4	27.4	1.2	2.2	2675.4	27.4
G10	89.8	146.9	0.85	0.4970	0.0060	12.8437	0.1990	0.1875	0.0028	2600.9	51.8	2668.3	36.3	2720.4	28.3	2.5	4.4	2720.4	28.3
G11	30.3	55.9	0.38	0.4925	0.0060	12.8181	0.2009	0.1888	0.0029	2581.6	51.7	2666.4	36.6	2731.9	28.8	3.2	5.5	2731.9	28.8
G12	39.9	68.5	0.45	0.5124	0.0061	13.3968	0.2037	0.1897	0.0028	2666.8	52.3	2708.0	35.8	2739.6	27.8	1.5	2.7	2739.6	27.8
G13	45.9	78.3	0.55	0.5060	0.0060	13.1689	0.1985	0.1888	0.0027	2639.5	51.7	2691.8	35.5	2732.1	27.5	1.9	3.4	2732.1	27.5
G14	89.5	155.3	0.49	0.5060	0.0059	13.2594	0.1868	0.1901	0.0025	2639.7	50.3	2698.3	33.4	2743.1	25.3	2.2	3.8	2743.1	25.3
G15	49.5	81.1	0.62	0.5132	0.0061	13.2343	0.1998	0.1871	0.0027	2670.2	52.1	2696.5	35.5	2717.0	27.5	1.0	1.7	2717.0	27.5
G16	133.5	229.4	0.55	0.5034	0.0059	12.9752	0.1852	0.1870	0.0025	2628.3	50.3	2677.9	33.8	2716.1	25.7	1.8	3.2	2716.1	25.7
G17	143.6	461.6	0.30	0.2986	0.0034	4.2819	0.0608	0.1040	0.0014	1684.5	34.1	1689.9	29.1	1697.4	22.2	0.3	0.8	1697.4	22.2
G18	72.6	118.9	0.62	0.5181	0.0061	13.8887	0.2014	0.1945	0.0027	2690.9	51.6	2742.1	34.4	2780.8	26.3	1.9	3.2	2780.8	26.3
G19	57.6	103.5	0.30	0.5071	0.0063	12.8199	0.2159	0.1835	0.0030	2644.0	54.1	2666.5	38.9	2684.3	31.1	0.8	1.5	2684.3	31.1
G20	111.9	362.3	0.10	0.3144	0.0037	5.0467	0.0800	0.1165	0.0018	1762.3	36.4	1827.2	32.7	1902.7	26.3	3.6	7.4	1902.7	26.3
G21	69.5	124.5	0.40	0.4993	0.0059	12.5234	0.1850	0.1820	0.0026	2610.6	50.6	2644.5	34.6	2671.2	26.6	1.3	2.3	2671.2	26.6
G22	68.9	109.1	0.62	0.5287	0.0064	13.7951	0.2130	0.1893	0.0028	2735.8	53.6	2735.7	36.2	2736.4	28.2	0.0	0.0	2736.4	28.2
G23	77.3	146.9	0.29	0.4899	0.0057	12.6140	0.1842	0.1868	0.0026	2570.2	49.7	2651.3	34.2	2714.5	26.3	3.1	5.3	2714.5	26.3

G24	10.6	208.4	0.72	0.0449	0.0006	0.3158	0.0117	0.0511	0.0019	282.8	7.5	278.7	19.4	245.3	16.3	-1.5	-15.3	282.8	7.5
G25	13.2	288.1	0.63	0.0412	0.0005	0.2927	0.0089	0.0515	0.0016	260.3	6.6	260.6	15.2	264.6	14.2	0.1	1.6	260.3	6.6
G26	9.0	191.6	0.82	0.0403	0.0006	0.2827	0.0119	0.0509	0.0022	254.8	7.2	252.8	20.1	235.9	17.9	-0.8	-8.0	254.8	7.2
G27	208.9	339.9	0.31	0.5560	0.0065	16.4409	0.2358	0.2146	0.0029	2849.9	53.6	2902.8	34.3	2940.5	26.1	1.8	3.1	2940.5	26.1
G28	167.9	327.3	0.43	0.4660	0.0054	11.6545	0.1682	0.1815	0.0025	2466.2	47.6	2577.1	33.5	2666.2	25.7	4.3	7.5	2666.2	25.7
G29	55.5	86.7	0.96	0.5057	0.0061	13.1276	0.2055	0.1884	0.0028	2638.2	52.0	2688.9	36.4	2727.9	28.5	1.9	3.3	2727.9	28.5
G30	97.7	159.5	0.66	0.5155	0.0060	13.6183	0.2020	0.1917	0.0027	2680.1	51.4	2723.5	34.7	2756.7	26.8	1.6	2.8	2756.7	26.8
G31	43.1	113.3	0.47	0.3468	0.0042	5.9547	0.1002	0.1246	0.0020	1919.4	39.9	1969.2	35.3	2022.7	28.7	2.5	5.1	2022.7	28.7
G32	104.2	184.6	0.28	0.5177	0.0061	13.7135	0.2031	0.1922	0.0027	2689.5	51.5	2730.1	34.7	2761.1	26.7	1.5	2.6	2761.1	26.7
G33	76.7	110.5	1.00	0.5331	0.0064	14.1278	0.2209	0.1923	0.0029	2754.5	53.7	2758.3	36.4	2761.8	28.5	0.1	0.3	2761.8	28.5
G34	84.5	134.3	0.41	0.5576	0.0066	16.6879	0.2510	0.2172	0.0031	2856.7	54.5	2917.1	35.6	2959.8	27.6	2.1	3.5	2959.8	27.6
G35	42.1	68.5	0.77	0.5043	0.0062	13.0330	0.2147	0.1875	0.0030	2632.1	52.7	2682.0	37.9	2720.7	30.2	1.9	3.3	2720.7	30.2
G36	74.1	162.2	0.23	0.4468	0.0053	11.7555	0.1828	0.1909	0.0029	2381.0	47.3	2585.1	35.7	2750.0	28.3	7.9	13.4	2750.0	28.3
G37	70.0	111.9	0.77	0.5140	0.0063	13.6441	0.2267	0.1926	0.0031	2673.7	53.6	2725.3	38.3	2764.6	30.5	1.9	3.3	2764.6	30.5
G38	111.1	205.6	0.36	0.4922	0.0058	12.7903	0.1932	0.1885	0.0027	2580.3	49.9	2664.3	34.9	2729.5	27.2	3.2	5.5	2729.5	27.2
G39	22.9	64.3	1.07	0.2834	0.0036	4.1095	0.0862	0.1052	0.0022	1608.4	36.2	1656.2	39.8	1718.3	34.5	2.9	6.4	1718.3	34.5
G40	159.8	304.9	0.43	0.4823	0.0056	12.8045	0.1928	0.1926	0.0028	2537.4	48.9	2665.4	34.8	2764.7	27.2	4.8	8.2	2764.7	27.2
G41	78.0	218.2	0.50	0.3250	0.0038	5.1918	0.0847	0.1159	0.0018	1814.1	37.4	1851.3	33.5	1894.1	26.9	2.0	4.2	1894.1	26.9
G42	139.0	242.0	0.28	0.5249	0.0062	14.0342	0.2182	0.1940	0.0029	2719.8	52.3	2752.0	35.9	2776.5	28.2	1.2	2.0	2776.5	28.2
G43	144.1	286.7	0.56	0.4531	0.0053	11.9810	0.1856	0.1919	0.0028	2408.9	47.3	2602.9	35.4	2758.3	28.1	7.5	12.7	2758.3	28.1
G44	115.4	261.6	0.12	0.4420	0.0052	11.1959	0.1768	0.1838	0.0028	2359.7	46.8	2539.6	35.8	2687.3	28.5	7.1	12.2	2687.3	28.5
G45	19.7	47.6	0.45	0.3762	0.0050	6.7594	0.1477	0.1304	0.0028	2058.3	46.7	2080.4	45.1	2103.2	38.7	1.1	2.1	2103.2	38.7
G46	47.6	110.5	0.96	0.3467	0.0043	5.5366	0.1038	0.1159	0.0021	1919.0	40.9	1906.3	38.1	1893.3	31.5	-0.7	-1.4	1893.3	31.5
G47	90.5	235.0	0.59	0.3406	0.0041	5.5027	0.0939	0.1172	0.0019	1889.3	39.1	1901.0	35.1	1914.6	28.5	0.6	1.3	1914.6	28.5
G48	30.3	76.9	0.61	0.3452	0.0045	5.4885	0.1189	0.1154	0.0025	1911.4	42.9	1898.8	43.3	1885.8	37.0	-0.7	-1.4	1885.8	37.0
G49	88.7	162.2	0.36	0.4991	0.0061	13.2681	0.2280	0.1929	0.0032	2609.8	52.6	2698.9	39.1	2767.1	31.7	3.3	5.7	2767.1	31.7
G50	255.6	482.5	0.30	0.4900	0.0057	12.5829	0.1956	0.1863	0.0028	2570.8	49.4	2648.9	35.5	2709.9	28.0	2.9	5.1	2709.9	28.0
G51	11.0	29.4	0.22	0.3615	0.0050	6.0796	0.1476	0.1220	0.0030	1989.2	46.9	1987.3	48.7	1986.1	42.4	-0.1	-0.2	1986.1	42.4
G52	95.2	155.3	0.54	0.5223	0.0062	13.4814	0.2220	0.1873	0.0030	2708.9	52.6	2714.0	37.4	2718.5	29.9	0.2	0.4	2718.5	29.9
G53	181.4	306.3	0.43	0.5231	0.0061	13.9677	0.2232	0.1937	0.0030	2712.3	52.0	2747.5	36.5	2774.2	29.0	1.3	2.2	2774.2	29.0

G54	126.7	215.4	0.61	0.4948	0.0059	11.6366	0.1961	0.1706	0.0028	2591.6	51.1	2575.6	37.7	2563.8	30.3	-0.6	-1.1	2563.8	30.3
G55	52.2	145.5	0.27	0.3436	0.0041	5.6066	0.1002	0.1184	0.0021	1903.9	39.7	1917.1	36.5	1932.2	30.1	0.7	1.5	1932.2	30.1
G56	7.4	14.0	0.22	0.5005	0.0084	13.5315	0.3900	0.1962	0.0058	2615.9	72.4	2717.5	64.1	2794.7	55.9	3.7	6.4	2794.7	55.9
G57	69.1	114.7	0.25	0.5466	0.0066	15.0746	0.2559	0.2001	0.0033	2811.1	54.9	2820.0	38.7	2827.0	31.1	0.3	0.6	2827.0	31.1
G58	80.0	124.5	0.87	0.5127	0.0062	13.3730	0.2286	0.1893	0.0031	2668.3	52.6	2706.4	38.6	2735.7	31.2	1.4	2.5	2735.7	31.2
G59	90.2	240.6	0.63	0.3280	0.0039	5.2967	0.0922	0.1172	0.0020	1828.5	38.0	1868.3	35.2	1913.7	29.0	2.1	4.4	1913.7	29.0
G60	232.3	430.8	0.26	0.5020	0.0059	13.1977	0.2170	0.1908	0.0030	2622.3	50.6	2693.9	37.1	2748.8	29.8	2.7	4.6	2748.8	29.8
G61	285.6	595.8	0.05	0.4759	0.0056	12.0270	0.1979	0.1834	0.0029	2509.3	48.8	2606.5	36.9	2683.6	29.7	3.7	6.5	2683.6	29.7
G62	67.6	106.3	0.54	0.5399	0.0066	14.8489	0.2600	0.1996	0.0034	2782.9	54.8	2805.6	39.6	2822.7	32.3	0.8	1.4	2822.7	32.3
G63	19.7	36.4	0.37	0.4938	0.0065	12.9942	0.2625	0.1909	0.0038	2587.1	55.8	2679.2	45.0	2750.2	37.8	3.4	5.9	2750.2	37.8
G64	84.0	162.2	0.49	0.4563	0.0056	10.2562	0.1856	0.1631	0.0029	2423.4	49.2	2458.2	39.5	2487.7	32.5	1.4	2.6	2487.7	32.5
G65	12.4	32.2	0.32	0.3591	0.0055	6.0101	0.1814	0.1214	0.0037	1977.9	51.9	1977.3	59.6	1977.5	53.3	0.0	0.0	1977.5	53.3
G66	356.9	693.8	0.05	0.5068	0.0060	13.6432	0.2297	0.1953	0.0032	2642.7	51.1	2725.3	37.8	2787.7	30.6	3.0	5.2	2787.7	30.6
G67	80.3	124.5	0.75	0.5270	0.0064	14.2360	0.2531	0.1960	0.0034	2728.8	53.9	2765.6	39.9	2793.1	32.7	1.3	2.3	2793.1	32.7
G68	122.3	237.8	0.26	0.4843	0.0058	12.7714	0.2228	0.1913	0.0032	2545.8	50.2	2662.9	38.8	2753.7	31.8	4.4	7.5	2753.7	31.8
G69	14.5	176.2	1.05	0.0659	0.0009	0.5061	0.0159	0.0557	0.0018	411.3	10.5	415.9	23.4	441.6	22.6	1.1	6.9	411.3	10.5
G70	32.1	50.4	0.99	0.4975	0.0064	12.7748	0.2533	0.1863	0.0036	2603.0	54.8	2663.2	43.8	2709.9	36.7	2.3	3.9	2709.9	36.7
G71	51.0	141.3	0.31	0.3426	0.0042	5.5187	0.1065	0.1169	0.0022	1899.0	40.2	1903.5	38.6	1909.0	32.4	0.2	0.5	1909.0	32.4
G72	61.4	114.7	0.43	0.4760	0.0058	11.1216	0.2073	0.1695	0.0031	2509.6	50.8	2533.4	40.7	2553.0	33.8	0.9	1.7	2553.0	33.8
G73	42.9	71.3	0.58	0.5144	0.0064	13.6049	0.2609	0.1919	0.0036	2675.2	54.7	2722.6	42.5	2758.5	35.5	1.7	3.0	2758.5	35.5
G74	36.1	111.9	0.28	0.3102	0.0039	4.6812	0.0961	0.1095	0.0022	1741.4	38.0	1763.9	39.7	1791.1	34.0	1.3	2.8	1791.1	34.0
G75	108.1	201.4	0.15	0.5103	0.0062	13.3803	0.2432	0.1902	0.0033	2657.8	52.5	2706.9	40.2	2744.2	33.3	1.8	3.1	2744.2	33.3

Osbornite

Table DR3: Comparative geochemistry of all known occurrences of TiVN together with chemistry of TiNbN samples at sites 1 and 2 on Skye.

	Ti0.77V0.28Fe0.77N Pure Osbornite*,	Osbornite like phase An Carnach Site 1	Osbornite An Carnach Site 1	Osbornite An Carnach Site 1	Osbornite Torrin Road Site 2	Osbornite Torrin Road Site 2	Wild comet Ti0.87V0.19Fe0.03N Chi M. et al., 2009**,
N	22.63	12.68	16.79	16.79	12.66	13.69	20.90
S		0.39	0.12	0.20	0.16	0.12	
Ti	77.37	57.77	42.09	46.59	61.3	61.8	62.15
V		2.13	2.88	3.20	14.8	14.48	14.44
Cr		4.42	3.32	4.26	0.1	0.88	
Fe		2.89	3.01	2.98	2.34	2.22	2.51
Nb		9.73	11	14.16	0.9	0.65	
C		11.61					
Total	100	101.62	79.21	88.18	92.26	93.84	100.00

Osbornite References

*Bannister, F. A., 1941, Osbornite meteoritic titanium nitride: Mineralogical Magazine, v. 26, p. 36-44.

**Chi, M., Ishii, H. A., Simon, S. B., Bradley, J. P., Dai, Z., Joswiak, D. J., Browning, N. D. and Matrajt, G., 2009, The origin of refractory minerals in comet 81P/WILD 2: Geochimica et Cosmochimica Acta, v. 73(12), p. 7150-7161, doi:10.1016 /j.gca.2009.08.033.

Barringerite

Table DR4: Comparative geochemistry of barringerite in selective meteorites, terrestrial Cu-Ni sulphides and the Skye impactoclastite sites.

	An Carnach Site 1	An Carnach Site 1	Torrin Road Site 2	Torrin Road Site 2		(Fe,Ni)2P *Buseck* 1969* **Meteorite Ollague**	*Brandstatter et al** 1991* **Meteorite Y-793274**
Si	0	0	0.36	0.5			
P	15.36	0	14.4	12.71	P	21.8	22.8
V	0	0	0.52	0.37	V		
Cr	2.97	4.43	0.36	0.23	Cr		0
Mn	2.26	2.22	0.61	0.92	Mn		
Fe	79.33	82.22	81.78	80.31	Fe	44.3	75.1
Ni	0.1	0.26	0.12	0.22	Ni	33.9	1.33
					Co	0.25	
Total	100.02	89.13	98.15	95.26	Total	100.25	0.21
							99.44

	*Chen et al 1994**** **Cu-Ni Sulphide, China**	*Zolenski et al 2008***** **Kaidun Meteorite (**FeCrP) Andreyivanovite- barringerite like phase
P	20.21	22.32
V	0.73	4
Cr	0.73	21.99
Mn		
Fe	76.22	46.27
Ni	2.85	2.54
Ti		2.79
Co	0	0.08
Total	100.01	99.99

At both sites barringerite has very low Ni concentrations (0.1 – 0.21 wt. %) but variable Fe, P, Cr, Mn and V. Such low Ni content is very similar to barringerite from the Y-793274 lunar meteorite (Brandstatter et al., 1991). However, Cr contents of Skye barringerite are closer to those of andreyivanovite (FeCrP) from the Kaidun meteorite (Zolenski et al., 2008).

Barringerite References

* Buseck. P. R., 1969, Phosphide from meteorites: Barringerite, a new iron-nickel mineral: Science v. 165, p. 169-17I

** Brandstätter, F., Koeberl, C. and Gerokuat, N., 1991,The discovery of iron barringerite in lunar meteorite Y-793274: Geochimica et Cosmochimica Acta, v. 55, p. 1173-1174.

*** Chen, K., Jin, Z. and Peng, Z., 1984, The discovery of iron barringerite (Fe,P) in China: Mineral. Abstracts, v. 35, p. 1871.

**** Zolensky, M., Gounelle, M., Mikouchi, T., Ohsumi, K., Le, L., Hagiya, K. and Tachikawa, O., 2008, Andreyivanovite: A second new phosphide from the Kaidun meteorite: American Mineralogist v. 93, p. 1295-1299, doi:10.2138/am.2008.2614.

Reidite

Table DR5: Raman peaks shown all meteorite impact studies (B-G) that have incorporated Raman analysis. Includes raman peaks from high pressure experimental data (A).

	A	*B*			*C*	*C*	*D*	*E*		*F*	*This*
Peak		*Stage II (35-45 Gpa)*	*Stage III (45-50 Gpa)*	*StageIV (>50 Gpa)*				*Level 3*	*Level 4*		*Study*
154	Reidite								157		
202	Zircon		*202*	*202*	*207*	*205*		200	201	202	202
214	Zircon			215				210	218		214
225	Zircon	*224*	*224*	*225*		*227*		224	221	225	228
	Reidite									238	
	Reidite				300					297	
	Reidite		327		330					327	
343	Reidite							342		353	
356	Zircon	*356*	*356*	*356*	*355*	*358*		352	351	356	352
393	Zircon							395			
	Reidite		404		407						
439	Zircon	*439*	*439*	*439*		*440*		436	433	439	433
	Reidite		465		462						
546	Zircon								549		548
552	Reidite		558		560						552
604	Reidite				611				607	610	
641	Zircon								638		638
840	Reidite		845		845		835		832	847	822
880	Reidite				885		879		870	887	868
							967				
974	Zircon	974	974	974		976	994	973	970	974	970
1001	Reidite							1001	1002	1001	1001
1008	Zircon	*1007*	*1007*	*1007*		*1008*	*1001*	1006		1008	1007

Reidite References

A. Knittle, E., and Williams, Q., 1993 High-pressure Raman spectroscopy of $ZrSiO_4$: Observation of the zircon to scheelite transition at 300 K: Am Mineral, v.78, p. 245–252.

B. Gucsik, A., 2006, 69th Annual meteoritical identification of reidite from the Reis impact crater using micro-raman spectroscopy: a review.

C. Chen, M., Yin, F., Li, X., Xie, X., Xiao, W., and Tan, D., 2013, Natural occurrence of reidite in the Xiuyan crater of China: Meteorics and Planetary Science, v. 48, p. 796-805, doi:10.1111/maps.12106.

D. Malone, L., Boonsue, S., Spray, J. and Wittman, A., 2010, Zircon-reidite relations in breccias from Chesapeake Bay impact: 41st Lunar and Planetary Science Conference.

E. Singleton, A. C., Osinski, G. R. and Shieh, S. R., 2015, Microscope effects of shock metamorphism in zircon from the Haughton impact structure, Canada: GSA special paper, v. 518, p. 135-148, doi:10.1130/2015.2518(09).

F. Gucsik, A., 2007, Micro-Raman spectroscopy of reidite as an impact-induced high pressure polymorph of zircon: Experimental investigation and attempt to application: Acta Mineralogica-Petrographica, Szeged 2006–2007, v. 47, p. 17-24.

G. This study.

Alabandite

Table DR6: Comparative geochemistry of alabandite in selective meteorites and the Skye impactoclastite sites.

	An Carnach Site 1	An Carnach Site 1	An Carnach Site 1	Torrin Rd, Site 2	Torrin Rd, Site 2	Torrin Rd, Site 2
Mn	61.78	59.47	61.67	58.59	54.85	42.03
Fe	1.52	0.00	0.00	0.00	0.00	31.36
Mg	0.1	0.23	0.15	0.00	0.05	0.04
Ca		4.19		9.67	7.87	0.00
Cr		1.19				
S	37.33	33.4	37.64	33.11	32.09	24.47

	Torrin Rd, Site 2	Torrin Rd, Site 2	Torrin Rd, Site 2	Torrin Rd, Site 2	Torrin Rd, Site 2		Ferroan alabandite **Meteorite Tupele (EL6)** **Dunlap et al., 2013*	Ferroan alabandite **Meteorite. EET 90102,** ***Fogel, 1997*
Mn	59.07	60.2	56.72	50.87	52.71	Mn	46.00	15.59
Fe	7.25	7.14	12.14	14.02	13.58	Fe	14.72	41.86
Mg	0.1	0.1	0.02	0	0.04	Mg	1.28	1.28
S	32.88	33.65	32.04	30.19	30.77	S	37.39	36.89
						Ca	0.19	2.24
						Cr	0.42	2.11
Total %	99.3	101.09	100.92	95.08	97.1	Total	100.00	99.97

Alabandite References

***** Dunlap, D. R., Pewit, M. L.,; McSween, H. Y., Taylor, L. A. and Doherty, R., 2013, Tupelo: A new EL6 Enstatite Chondrite: 44th Lunar and Planetary Science Conference, abstract 2088.

*Fogel, R. A., 1997, On the significance of diopside and oldhamite in enstatite chondrites and aubrites: Meteoritics and Planetary Science, v. 32, p. 577–591.

Table DR7: Site 2 (Chambered Cairn- lower unit) zircon ages

Zircon	207Pb/206Pb age	± 2 sigma	Discordance
1	1819.9	27.8	1.8
2	1737.9	3.4	0.2
3	1340.4	3.7	-1.5
4	1111.8	13.8	-4.3
5	1489.8	18.2	-1.9
6	1492.4	12.3	-0.8
7	1633.2	15.1	-1.9
8	3227.1	3.1	-3.7
9	3219.4	2.5	-1.1
10	1765.9	6.0	0.4
11	2826.0	6.0	0.4
12	2813.6	3.1	0.8
13	1179.3	9.5	-0.9
14	1720.1	8.3	0.9
15	1728.7	6.2	-3.0
16	1719.7	6.2	1.1

Native Iron

Table DR8: Chemistry of native iron within sites 1 and 2 on Skye.

	Native metal An Carnach Site 1	Native metal Torrin Rd, Site 2	Native metal Torrin Rd, Site 2	Native metal Torrin Rd, Site 2	Minimum	Maximum
Si	1.55	0.8	1.45	2.31	0.8	2.31
Cr	0.88	0.27	1.07	0.29	0.27	1.07
Mn	1.23	0.1	1.37	0.66	0.1	1.37
Fe	92.06	93.09	92.24	92.09	92.06	93.09
Ni	0.14	0.12	0.11	0.49	0.11	0.49
Cu	2.56	3.66	2.42	2.84	2.42	3.66
C	1.12	2.18				
Total %	100.54	100.22	98.66	98.68	95.76	101.99